

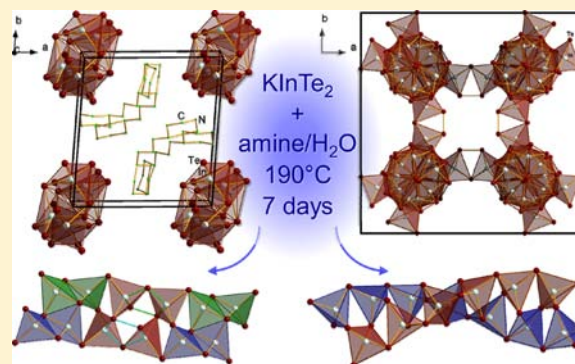
Synthesis of Complex Polymeric Telluridoindates from  $\text{KInTe}_2$ 

Johanna Heine, Silke Santner, and Stefanie Dehnen\*

Fachbereich Chemie and Wissenschaftliches Zentrum für Materialwissenschaften (WZMW), Philipps-Universität Marburg, 35037 Marburg, Germany

## Supporting Information

**ABSTRACT:** Four new polymeric telluridoindates  $[\text{K}(\text{18-crown-6})][\text{InTe}_2] \cdot 2en$  (**1**) (18-crown-6 = 1,4,7,10,13,16-hexaoxacyclooctadecane),  $[\text{K}([\text{2.2.2}]\text{crypt})]_2[\text{In}_2\text{Te}_6] \cdot 0.5en$  (**2**) ([2.2.2]crypt = 4,7,13,16,21,24-hexaoxa-1,10-diazabicyclo[8.8.8]hexacosane),  $[\text{HTMDP}]_2[\text{In}_4\text{Te}_8]$  (**3**) (TMDP = 4,4'-trimethylenedipiperidine), and  $[\text{HDAP}]_8[\text{In}_{12}\text{Te}_{23}]$  (**4**) (DAP = 1,3-diaminopropane) were prepared from  $\text{KInTe}_2$  as a starting material. With  $[\text{InTe}_4]$  tetrahedra as the primary building unit in all four compounds, there is a significant increase in complexity in going from the simple chain-like anionic structures in **1** and **2** to an intricate band-type anion in **3** and finally an anionic framework with lig-topology in **4**.



## INTRODUCTION

The heavier congeners of silicates and borates have long been in the focus of researchers trying to combine the porous nature of zeolites with semiconducting properties.<sup>1</sup> Open framework thioindates are an interesting subclass of these materials. Following the early examples of Yaghi<sup>2</sup> and Parise,<sup>3</sup> a large variety of new porous compounds have been synthesized<sup>4</sup> with properties such as ion conductivity,<sup>5</sup> photoluminescence,<sup>6</sup> and photocatalytic activity.<sup>7</sup> Although formally analogous to the lighter homologues, the porosity of these materials is not generated via the formation of rings and cages from  $[\text{ME}_4]$  (M = metal; E = chalcogen) units, but stems from the linking of supertetrahedral clusters.

Although many examples of porous thioindates are known, the corresponding selenidoindates<sup>8</sup> and telluridoindates<sup>9</sup> have remained rare.

Most chalcogenidoindates, from low dimensional to open framework materials, have been synthesized by reacting the elements or binary precursors with amines at elevated temperature. The amines, either in protonated form or as metal complexes such as  $[\text{M}(\text{en})_3]^{n+}$  (en = ethylenediamine; n = charge) act as templates during the formation of extended anionic chalcogenidoindates, influencing the resulting structure.<sup>10</sup> Yet, the structure formation is not only controlled by template effects but also by the nature and ratio of starting materials, as is exemplified in the system Zn/en/In/Te<sup>11</sup> and by the ability of some amines to coordinate to indium atoms of the anionic substructure.<sup>12</sup>

We have employed  $\text{KInTe}_2$ ,<sup>13</sup> a phase comprising chains of edge-sharing  $[\text{InTe}_4]$  tetrahedra that are separated and stabilized by potassium ions, as a starting material for extraction and aminothermal reactions under different conditions, resulting in four new compounds:  $[\text{K}(\text{18-crown-6})][\text{InTe}_2] \cdot 2en$  (**1**) (18-crown-6 = 1,4,7,10,13,16-hexaoxacyclooctadecane),

$[\text{K}([\text{2.2.2}]\text{crypt})]_2[\text{In}_2\text{Te}_6] \cdot 0.5en$  (**2**) ([2.2.2]crypt = 4,7,13,16,21,24-hexaoxa-1,10-diazabicyclo[8.8.8]hexacosane),  $[\text{HTMDP}]_2[\text{In}_4\text{Te}_8]$  (**3**) (TMDP = 4,4'-trimethylenedipiperidine), and  $[\text{HDAP}]_8[\text{In}_{12}\text{Te}_{23}]$  (**4**) (DAP = 1,3-diaminopropane). While **1**–**3** contain one-dimensional anionic structures, **4** represents an anionic framework telluridoindate.

## EXPERIMENTAL SECTION

**General.** The synthesis of **1** and **2** was performed under an Ar atmosphere. Ethylenediamine and toluene were freshly distilled from calcium hydride and sodium, respectively, prior to use. 1,4,7,10,13,16-Hexaoxacyclooctadecane (18-crown-6) and 4,7,13,16,21,24-hexaoxa-1,10-diazabicyclo[8.8.8]-hexacosane ([2.2.2]crypt) were dried under vacuum for several hours before use.  $\text{KInTe}_2$  was prepared according to the literature procedure.<sup>13</sup> 4,4'-Trimethylenedipiperidine (TMDP) and 1,3-diaminopropane (DAP) were used as received from commercial sources.

**Synthesis of  $[\text{K}(\text{18-crown-6})][\text{InTe}_2] \cdot 2en$  (**1**) and  $[\text{K}([\text{2.2.2}]\text{crypt})]_2[\text{In}_2\text{Te}_6] \cdot 0.5en$  (**2**).** A mixture of 50 mg of  $\text{KInTe}_2$  (0.122 mmol, 1 equiv) and 32 mg of 18-crown-6 (0.122 mmol, 1 equiv) or 46 mg of [2.2.2]crypt (0.122 mmol, 1 equiv) was suspended in 10 mL of en for 3 h. The resulting deep red solutions were left undisturbed for 12 h. The solutions were decanted via a cannula from any remaining solids, and the resulting clear solutions were layered with toluene in 1:1 ratio. After several days, **1** and **2** crystallized as light yellow needles along with significant amounts of powdery byproducts. The yield of the crystalline material upon hand-separation from the powder was ca. 66% (65 mg, 0.08 mmol with respect to  $\text{KInTe}_2$ ) for **1** and ca. 80% (31 mg, 0.03 mmol with respect to  $\text{KInTe}_2$ ) for **2**. The products were weighed out, and yields were calculated based on semidried product. Powder XRD measurements and CHN analyses revealed decomposition of the compounds upon drying.

Received: November 29, 2012

Published: March 27, 2013

Table 1. Data of the Single-Crystal X-ray Diffraction Analyses of Compounds 1–4

compound	1	2	3	4
empirical formula	C <sub>16</sub> H <sub>40</sub> In K N <sub>4</sub> O <sub>6</sub> Te <sub>2</sub>	C <sub>19</sub> H <sub>40</sub> In K N <sub>3</sub> O <sub>6</sub> Te <sub>3</sub>	C <sub>26</sub> H <sub>54</sub> In <sub>4</sub> N <sub>4</sub> Te <sub>8</sub>	C <sub>24</sub> H <sub>88</sub> In <sub>12</sub> N <sub>16</sub> Te <sub>23</sub>
<i>F</i> <sub>w</sub> (g mol <sup>-1</sup> )	793.64	943.26	1902.81	8625.28
crystal color/shape	yellow needle	yellow needle	orange needle	orange needle
crystal size (mm <sup>3</sup> )	0.30 × 0.10 × 0.01	0.18 × 0.06 × 0.01	0.10 × 0.05 × 0.04	0.33 × 0.07 × 0.02
radiation, λ (Å)	Mo K <sub>α</sub> , 0.71073	Mo K <sub>α</sub> , 0.71073	Mo K <sub>α</sub> , 0.71073	Mo K <sub>α</sub> , 0.71073
crystal system	monoclinic	monoclinic	triclinic	tetragonal
space group	<i>C</i> 2/ <i>c</i>	<i>P</i> 2 <sub>1</sub> / <i>c</i>	<i>P</i> $\bar{1}$	<i>I</i> $\bar{4}$ <i>m</i> 2
<i>a</i> (Å)	23.528(5)	15.254(3)	12.355(3)	27.762(13)
<i>b</i> (Å)	17.080(3)	26.260(5)	14.059(3)	27.762(13)
<i>c</i> (Å)	7.3860(15)	8.0687(16)	15.128(3)	36.444(11)
α (deg)	90	90	68.91(3)	90
β (deg)	95.83(3)	101.68(3)	73.34(3)	90
γ (deg)	90	90	79.92(3)	90
<i>V</i> (Å <sup>3</sup> )	2952.8(10)	3165.3(11)	2341.1(10)	28088(20)
<i>Z</i>	4	4	2	4
ρ <sub>calcd</sub> (g cm <sup>-3</sup> )	1.785	1.979	2.699	2.040
μ (Mo Kα) (mm <sup>-1</sup> )	2.91	3.621	6.852	6.615
absorp corr type	Gaussian	numerical	Gaussian	numerical
min/max transmission	0.5052/0.8973	0.6347/0.9208	0.6423/0.816	0.4012/0.8651
2θ max (deg)	53.48	53.48	53.44	53.62
reflms measured	16256	19559	20093	55026
<i>R</i> (int)	0.1374	0.2268	0.0874	0.1193
ind. reflns	3098	6572	9745	15468
ind. reflns ( <i>I</i> > 2σ( <i>I</i> ))	2515	2948	5694	2841
parameters	134	306	379	156
<i>R</i> <sub>1</sub> ( <i>I</i> > 2σ( <i>I</i> ))	0.0541	0.0949	0.0521	0.0732
<i>wR</i> <sub>2</sub> (all data)	0.145	0.2240	0.1068	0.1754
<i>S</i> (all data)	1.015	1.001	0.837	0.768
res. diff. peak/hole (e <sup>-</sup> ·Å <sup>-3</sup> )	2.871/−1.123	1.918/−1.427	1.284/−1.312	1.580/−1.314

Table 2. Selected Bond Lengths, Interatomic Distances (in Å), and Angles (in deg) in Compounds 1–4, As Observed in the Crystal Structures

interatomic distance	1	2	3	4
In–Te	2.7881(6)–2.8028(6)	2.7472(8)–2.8059(5)	2.7264(6)–2.8852(8)	2.726(4)–2.841(4)
Te–In–Te	97.296(9)–120.521(6)	105.719(8)–112.177(8)	96.47(5)–121.93(6)	103.29(11)–116.61(13)
Te–Te		2.7279(7)	2.8577(7)	2.812(7)
In...In	3.6938(7)	4.0790(8)	3.6318(9)–4.2048(9)	3.9443(35)–4.4158(41)

**Synthesis of [HTMDP]<sub>2</sub>[In<sub>4</sub>Te<sub>8</sub>] (3) and [HDAP]<sub>8</sub>[In<sub>12</sub>Te<sub>23</sub>] (4).** A mixture of 100 mg of KInTe<sub>2</sub> (0.244 mmol), 1 g of TMDP or 1 mL of DAP, and 2 mL of H<sub>2</sub>O were mixed and transferred into a Teflon-lined steel autoclave of 25 mL volume. The reaction mixtures were heated at 190 °C for seven days. The raw products were transferred into a Schlenk vessel, shortly degassed, and kept under an inert atmosphere. Compounds 3 and 4 were obtained as light orange needles along with black powdery byproduct containing elemental tellurium. The yield of the crystalline material upon hand-separation from the powder was ca. 59% (68 mg, 0.04 mmol with respect to KInTe<sub>2</sub>) for 3 and ca. 35% (61 mg, 0.01 mmol with respect to KInTe<sub>2</sub>) for 2. The products were weighed out, and yields were calculated based on semidried product. Powder XRD measurements and CHN analyses revealed decomposition of the compounds upon drying.

**Verification of Reproducibility and Phase Purity.** Because of the difficulties with dry isolation of the compounds, single-crystal XRD measurements were performed on many different crystals from many different batches of each of the title compounds. The results showed only compounds 1–4 to be present in the samples, thus indicating phase purity for the obtained single-crystalline material.

**Single-Crystal X-ray Diffraction.** Data were collected on a diffractometer equipped with a STOE imaging plate detector system IPDS2, using graphite-monochromized Mo K<sub>α</sub> radiation (λ = 0.71073

Å) at 100 K. Structure solution and refinement were performed by direct methods and full-matrix least-squares on *F*<sup>2</sup>, respectively, using ShelxTL software.<sup>14</sup> Tables 1 and 2 summarize the crystallographic data and selected interatomic distances and angles for 1–4. Details on the structure solution and refinement: 1, refinement of C, O, K, In, and Te atomic positions employing anisotropic displacement parameters except for the positions of two disordered *en* molecules, which were isotropically refined with half occupancy. H atom positions of the crown ether molecule were implemented via a riding model, and H atom positions of the disordered solvent were not calculated; 2, refinement of C, O, N, K, In, and Te atomic positions employing anisotropic displacement parameters except for the positions of an *en* molecule, which was isotropically refined with half occupancy. H atom positions of the cryptand and *en* molecule were implemented via a riding model, except for the H atom positions of the amine groups, which were not calculated. The very thin, needle-like habit of the crystals has precluded us from collecting a data set of very good quality in this case; 3, refinement of C, N, In, and Te atomic positions employing anisotropic displacement parameters. H atom positions were implemented via a riding model. The position of the protonated secondary amine group in the TMDP molecules is disordered due to crystallographic symmetry and was thus modeled by half occupancy of all involved H atoms; 4, refinement of In and Te atomic positions employing anisotropic displacement parameters. The contents of the

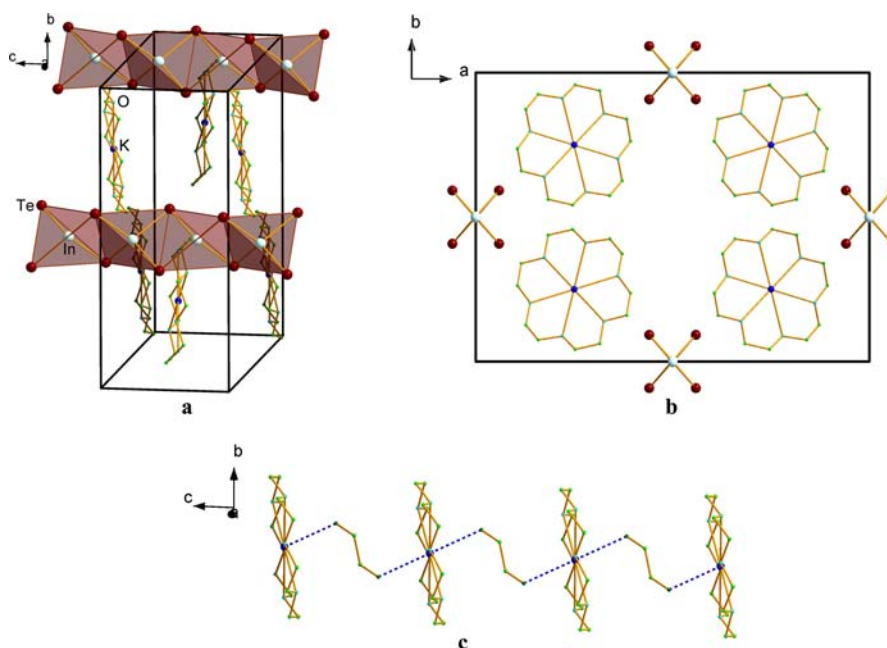


**Figure 1.** Different views of a fragment of the crystal structure (a,b) and detailed view of a cationic chain (c) in **1**.

anionic framework were modeled using the SQUEEZE algorithm as implemented in the software package PLATON.<sup>15</sup>

**UV–Visible Spectra.** UV–vis spectra were recorded on a Perkin-Elmer Cary 5000 UV/vis/NIR spectrometer in the range of 800–200 nm, employing double beam technique. The samples were prepared as suspensions of as-prepared single-crystals, freshly gathered from the mother liquid, in nujol oil, and were brought into the UV–vis beam between two quartz plates.

## RESULTS AND DISCUSSION

**Syntheses.** Compounds **1** and **2** were prepared by extracting  $\text{KInTe}_2$  with *en* in the presence of equimolar amounts of the respective potassium sequestering agent. The resulting bright red solutions were filtered to remove any traces of undissolved starting material and layered with toluene. After 5–7 days, yellow crystals of **1** and **2** appear among yellowish powdery byproducts. While **1** represents a diluted homologue of the starting material  $\text{KInTe}_2$ , upon complexation of  $\text{K}^+$  cations by 18-crown-6 molecules and incorporation of solvent *en* molecules, an oxidation reaction is necessary to accomplish the formation of the **2**. This may be facilitated by the use of cryptand, such as Schrobilgen and co-workers have shown for the oxidation of  $[\text{Pb}_9]^{4+}$  to  $[\text{Pb}_9]^{3+}$  in *en* solution.<sup>16</sup>

We also noted that while the crystallization of **1** and **2** is obviously controlled by the addition of the cation capturing agents, these are not necessary to dissolve  $\text{KInTe}_2$  in *en*. This has prompted us to expand the reaction conditions toward aminothermal methods where the preformed telluridoindate fragments in solution might result in extended architectures unavailable via the dissolution of the elements or binaries.

Compounds **3** and **4** were prepared by treating  $\text{KInTe}_2$  with a mixture of the respective amine (TMDP or DAP, respectively) and water at a temperature of 190 °C for seven days in a Teflon-lined steel autoclave. Both compounds can be obtained from the reaction mixtures as thick orange needles. Reactions at temperatures below 190 °C did not prove successful. The addition of water to the reaction mixture is necessary to enable the formation of ammonium ions that act as templates as well as counterions for the extended tellur-

idoindate anions. We have also tested the influence of the In/Te source on the reaction outcome by using the same reaction conditions as for the synthesis of **3** and **4**, but employing elemental indium and tellurium at a 1:2 ratio as in the original starting material  $\text{KInTe}_2$ . Using the synthesis conditions of **3**, we obtained no single crystalline material. Using the conditions of **4**, we obtained the known compound UCR-2 containing the anionic framework telluridoindate  $[\text{In}_{33}\text{Te}_{56}]^{13-}$ .<sup>8b</sup>

The reactions show moderate to good yields, and they are well-reproducible. However, an intrinsic problem, especially for the application of further analytical techniques, is the fast decomposition upon isolation from any liquid. We were only in the position to characterize wet crystals, either freshly gathered from the mother liquor or from the washing agent; thus, CHN analyses or powder XRD measurements could not be performed. Thus, the phase purity was checked by multiple single-crystal diffraction experiments on various crystals from different batches, which never showed anything else but the reported products. Powdery byproducts turned out to be unidentifiable or were identified as being elemental tellurium (see Experimental Section).

**Crystal Structures.** All compounds were structurally characterized by means of single-crystal X-ray diffraction (see the Experimental Section).

Compound **1** crystallizes in the monoclinic space group  $C2/c$  (No. 15). Its anionic part, a chain comprising edge-sharing  $[\text{InTe}_4]$  tetrahedra, is similar to the starting material  $\text{KInTe}_2$  and a number of solvothermally prepared telluridoindates.<sup>17</sup> In contrast to some of these literature examples, the chains in **1** experience no wave-like distortion. The potassium ions in **1** are complexed by 18-crown-6 molecules and connected into chains parallel to the anionic ones via disordered *en* molecules. Different views of a fragment of the crystal structure, as well as details of the cationic chain, are provided in Figure 1. In short, **1** can be rationalized as a diluted variant of  $\text{KInTe}_2$ .

The anionic part of the structure of compound **2** is also formed by chains of  $[\text{InTe}_4]$  tetrahedra. Yet in **2**, which crystallizes in the monoclinic space group  $P2_1/c$  (No. 14), these



are not edge-sharing, but corner-sharing, and have an additional connection via a Te–Te bond. This anionic telluridoindate motif is already known from a number of compounds.<sup>18</sup> The chains are separated by potassium ions that are captured by [2.2.2]crypt and *en* molecules (Figure 2). As in **1**, the In/Te substructure in **2** shows very little overall distortion in contrast to some of the literature examples.

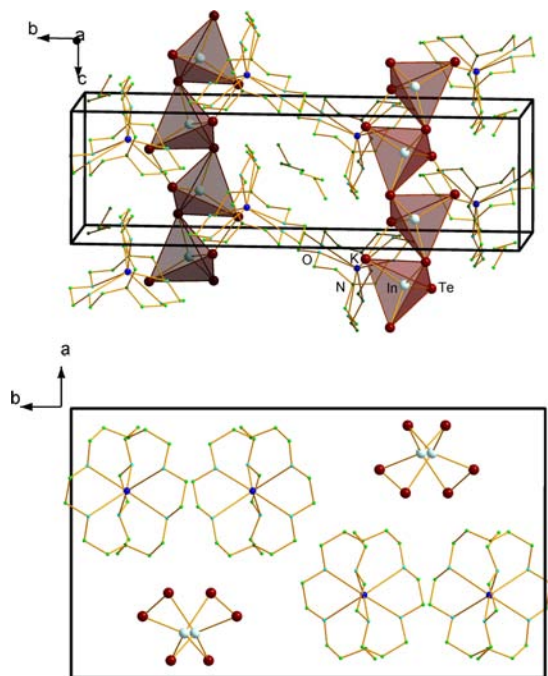


**Figure 2.** Different views of a fragment of the crystal structure of **2**.

Compound **3**, which crystallizes in the triclinic space group  $P\bar{1}$  (No. 2), shows a previously unknown anionic chain

structure. A clear way to understand the complex arrangement is to separate it into two smaller building units, each made up of four single  $[\text{InTe}_4]$  tetrahedra: the first unit represents a zigzag chain of edge-sharing tetrahedra. The second unit contains only corner-sharing tetrahedra that form a distorted pentagonal antiprismatic cavity through two additional Te–Te-bonds. Both building units are connected through corner-sharing at three Te atoms. A detailed view of this description is provided in Figure 3a. A view of a fragment of the overall structure is shown in Figure 3b. The anionic chains are separated by protonated TMDP molecules that form cationic, hydrogen-bonded chains (Figure 3c). This type of cation interaction has not been reported for TMDP so far, but for the related amine piperazine.<sup>19</sup>

Compound **4**, a framework telluridoindate, crystallizes in the tetragonal space group  $I\bar{4}m2$  (No. 119). Here, as for many framework structures with large cavities, only the rigid anionic part could be deduced from X-ray crystallography. The network is built up from helical double chains of  $[\text{InTe}_4]$  tetrahedra connected via  $[\text{In}_2\text{Te}_3]$  rings (Figure 4a and b, respectively). The helices run in  $c$  direction with a pitch of 36.444 Å, equal to the unit cell length  $c$ , with four connecting  $[\text{In}_2\text{Te}_3]$  rings branching off at 90° angles with respect to  $c$  and to each other. Four helices, two of each handedness, are found in one unit cell. These details are shown in Figure 4c,d. As a whole, the In/Te substructure accords to the **lig**-topology<sup>20</sup> (shown as an overlay in Figure 4e).

Occupying only 33% of the overall cell volume,<sup>15</sup> the anionic framework in this compound is much more open than the only previously known framework telluridoindate, UCR-2, that adopts the **srs**-topology and occupies 50% of the overall cell volume.<sup>9</sup> The framework in **4** is filled with protonated DAP and water molecules. As outlined above, it was not possible to determine the exact composition of the framework contents by means of other analytical methods due to decomposition of the compound upon drying.

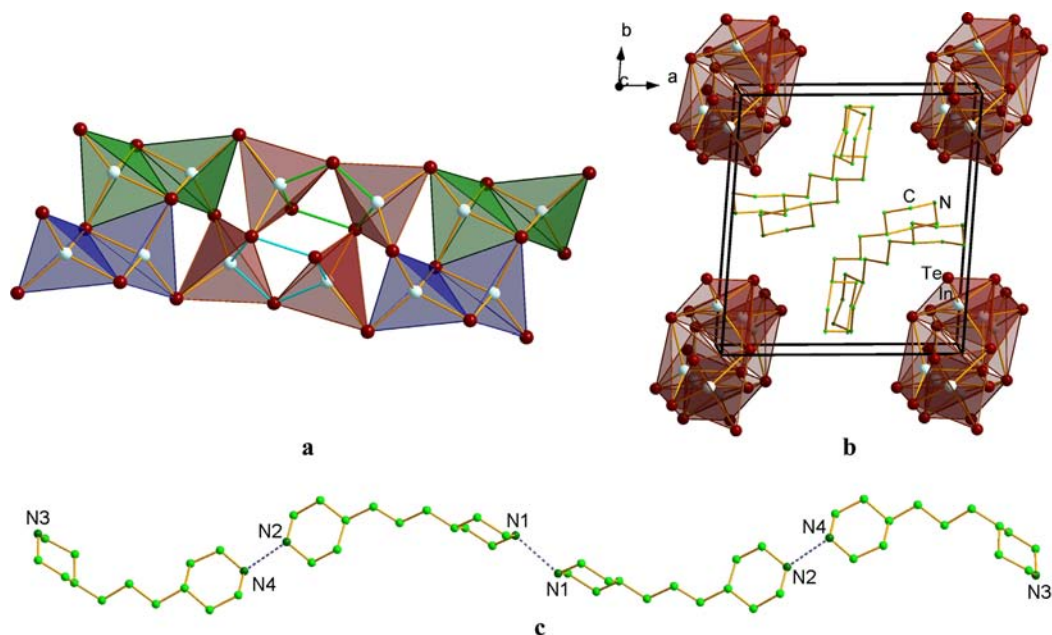


**Figure 3.** Representation of the anionic structural motif in **3**, highlighting the edge-sharing building unit by blue/green polyhedra, the corner-sharing building unit by red polyhedra, and the two pentagons by cyan/green bonds (a); a fragment of the crystal structure (b); and a view of the cationic chains of **3** (c).

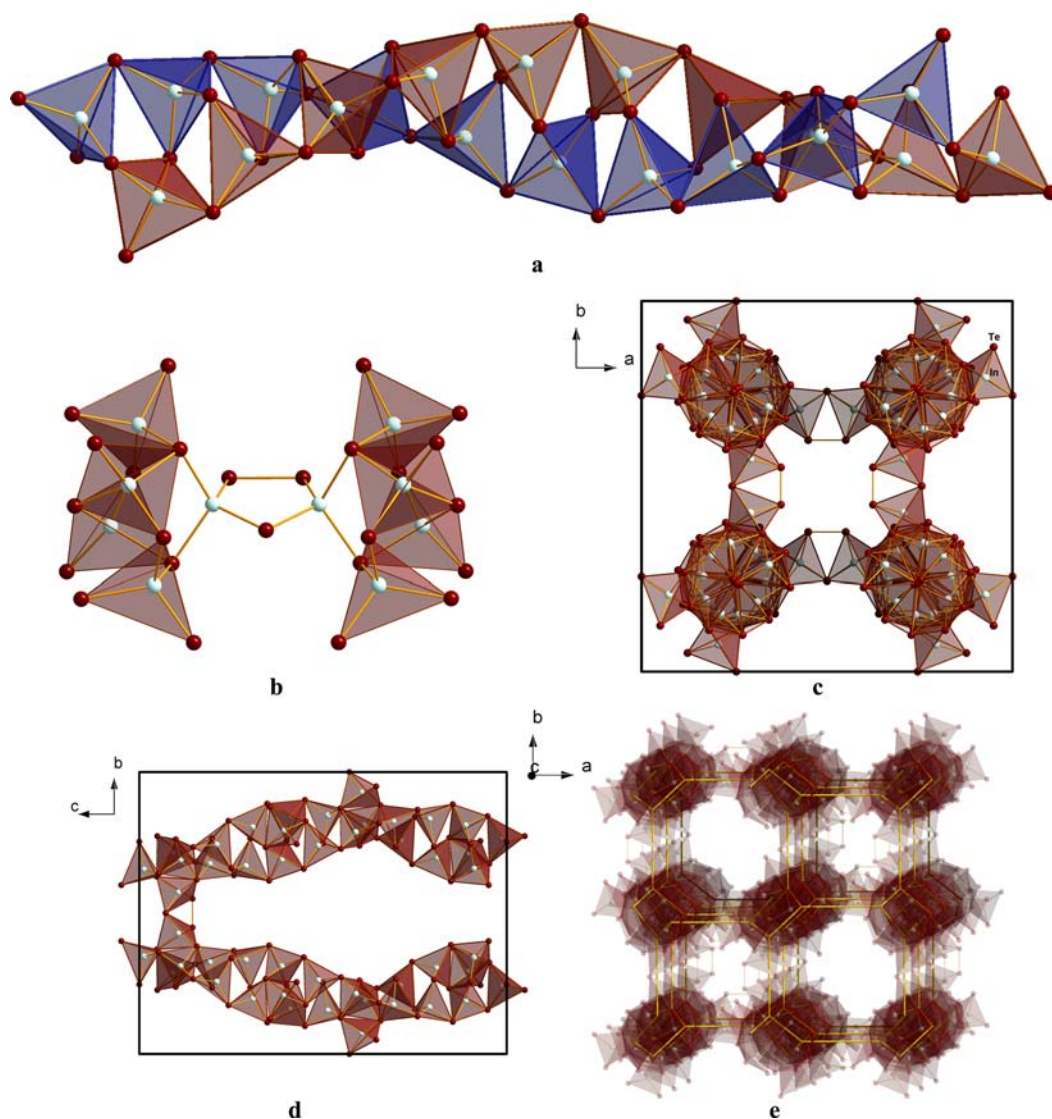


**Figure 4.** Color coded representation of the helical chains (a), the interconnecting  $[\text{In}_2\text{Te}_3]$ -rings (b), two different views of a fragment of the crystal structure (c,d), and a representation of the underlying lig-net (e) in 4.

The structures of **1–4** are all based on linked  $[\text{InTe}_4]$  tetrahedra, hereby showing corner-sharing or edge-sharing, or the combination of both. Whereas corner-sharing is the common linking mode of tetrahedra in the oxido-borates<sup>21</sup> or oxido-silicates,<sup>22</sup> edge-sharing, or the quoted combination of the linking modes, is more typical for nitrido-silicates<sup>23</sup> or the architectures of heavier chalcogenidometallates of Group 13 or 14.<sup>4,24</sup>

The architectures of the anionic frameworks of the title compound span a range in complexity. They lead from simple one-dimensional extension through more complex one-dimensional strands to complex and helical strands that are interconnected to form a three-dimensional network. The latter remind of borophosphate architectures that have also been observed as helical anions.<sup>25</sup> We assume that the increase in complexity comes along with the more drastic reaction conditions applied to the reactants in the case of the generation of compounds **3** and **4**. Room temperature procedures usually end up with simple topologies as those observed for **1** and **2**, whereas the combination of linking modes and the higher degree of interconnection is typical for high-temperature and/

or high-pressure techniques. This was also shown to an extreme extent for treatment of the lightest homologues of the title compounds, oxoborates, at extremely high pressures. A recent example is high-pressure  $\text{KB}_3\text{O}_5$  that combines corner-sharing  $[\text{BO}_3]$  and  $[\text{BO}_4]$  groups with edge-sharing  $[\text{BO}_4]$  tetrahedra upon preparation.<sup>26</sup>

**Optical Absorption Properties.** The structural properties observed in the title compounds are well reflected in their optical absorption behavior. Figure 5 shows the UV–visible spectra of suspensions of pulverized single-crystals of compounds **1–4** in nujol oil.

The UV–visible spectra of **1** and **2** do not differ significantly, according to a very similar architecture of the In/Te substructures that form one-dimensional strands of connected tetrahedra.  $E_{\text{onset}}$  is observed at 3.9 eV for both compounds, although one might suggest a slightly faster increase of the absorption in the case of **1**, according with the edge-sharing tetrahedra instead of corner-sharing ones in **2** that gives rise to a somewhat lesser density of the In/Te anion. Beside a notable redshift of the onset of absorption when going from **1** or **2** to **3** (smooth onset at 3 eV) and **4** ( $E_{\text{onset}} = 3.5$  eV), the differences

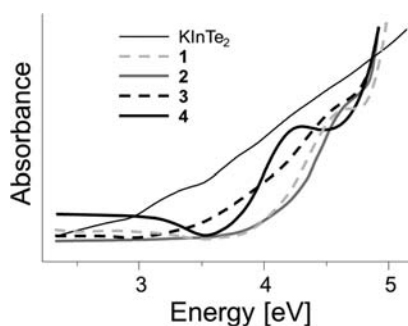


Figure 5. UV-visible spectra of suspensions of pulverized single-crystals of compounds 1–4 in nujol oil.

observed for 3 and 4 reflect the increasing density of the In/Te substructures that comes along with the higher complexity of the frameworks.

The optical absorption properties described above do not explain the observed colors of the single crystals; regarding the absorption behavior of the starting material  $\text{KInTe}_2$ ,<sup>13</sup> which forms deep red crystals, but shows no absorption below 2.5 eV, one recognizes that the absorption lines are consequently blue-shifted. This might point toward doping by small amounts of polytellurides. The formation of such species has been frequently observed upon extraction of binary or ternary tellurides, often accompanied by complex redox reactions.<sup>27</sup> Chalcogenidoindates are known for a distinct tendency for the formation of double or even triple salts, as well as for cocrystallization with chalcogenides and polychalcogenides.<sup>28</sup> Thus, the presence of small concentrations of polychalcogenides or other defects and impurities is likely to occur rather frequently here. This has been demonstrated through very detailed analysis of crystal compositions and colors for  $\text{LiInS}_2$ ,<sup>29</sup> and  $\text{LiInSe}_2$ ,<sup>30</sup> where crystal colors are highly dependent on preparation conditions, even for these simple chalcogenidoindates. Since polytellurides are usually intensely colored, doping can change the visual impression although not being detected by UV-visible spectroscopy beside the more prominent main phases. Another contribution to the mismatch of visible color and measured absorption energies might be a matter of particle size. Grinding of the samples indeed generates small particles of lighter color, such as observed for single-crystals of  $\text{LiGaTe}_2$ .<sup>31</sup>

## CONCLUSIONS

We have shown that the ternary phase  $\text{KInTe}_2$  may be used under different conditions as a starting material to generate new, more complex telluridoindates. Compounds 1 and 2 exemplify that  $\text{KInTe}_2$  can be extracted with amines under ambient conditions and that the resulting structures depend on the nature of the counterion complexes, as well as on the possibility of oxidation reactions to occur. Compound 3 is a rare example of a complex telluridoindate band-type anion. Compound 4 shows the second example containing an anionic framework telluridoindate. Unlike the known framework UCR-2, it exhibits the **lig**-topology and occupies only one-third of the overall cell volume of the compound.

We believe that ternary phases such as  $\text{KInTe}_2$  represent promising new starting materials in reactions toward new complex chalcogenidometallate materials. Our future studies will concentrate on the reactivity of phases such as  $\text{AlInSe}_2$ ,  $\text{AlInS}_2$ , and  $\text{AGaE}_2$  under ambient and solvothermal conditions

and on the structure directing influences of the chosen counterions and reaction conditions.

## ASSOCIATED CONTENT

### Supporting Information

CIF files for 1–4. Crystal and powder photographs. This material is available free of charge via the Internet at <http://pubs.acs.org>.

## AUTHOR INFORMATION

### Corresponding Author

\*(S.D.) E-mail: [dehnen@chemie.uni-marburg.de](mailto:dehnen@chemie.uni-marburg.de).

### Notes

The authors declare no competing financial interest.

## ACKNOWLEDGMENTS

We thank the Deutsche Forschungsgemeinschaft (DFG) for financial support of this work.

## REFERENCES

- (1) (a) Krebs, B. *Angew. Chem.* **1983**, *95*, 113–134; *Angew. Chem., Int. Ed.* **1983**, *22*, 113–134. (b) Bedard, R. L.; Wilson, S. T.; Vail, L. D.; Bennett, J. M.; Flanigen, E. M. In *Zeolites: Facts, Figures, Future*; Jacobs, P. A., van Santen, R. A., Eds.; Elsevier Science: Amsterdam, The Netherlands, 1989; Vol. 1, p 375. (c) Yaghi, O. M.; Sun, Z.; Richardson, D. A.; Groy, T. L. *J. Am. Chem. Soc.* **1994**, *116*, 807–808. (d) Rangan, K. K.; Trikalitis, P. N.; Kanatzidis, M. G. *J. Am. Chem. Soc.* **2000**, *122*, 10230–10231. (e) Kanatzidis, M. *Adv. Mater.* **2007**, *19*, 1165–1181.
- (2) Li, H.; Laine, A.; O’Keeffe, M.; Yaghi, O. M. *Science* **1999**, *283*, 1145–1147.
- (3) Cahill, C. L.; Ko, Y.; Parise, J. B. *Chem. Mater.* **1998**, *10*, 19–21.
- (4) For reviews, see: (a) Bu, X.; Zheng, N.; Feng, P. *Chem.—Eur. J.* **2004**, *10*, 3356–3362. (b) Feng, P.; Bu, X.; Zheng, N. *Acc. Chem. Res.* **2005**, *38*, 293–303. (c) Dehnen, S.; Melullis, M. *Coord. Chem. Rev.* **2007**, *251*, 1259–2167. (d) Vaqueiro, P. *Dalton Trans.* **2010**, *39*, 5965–5972. (e) Heine, J.; Dehnen, S. *Z. Anorg. Allg. Chem.* **2012**, *638*, 2425–2440.
- (5) Zheng, N.; Bu, X.; Feng, P. *Nature* **2003**, *426*, 428–432.
- (6) Zheng, N.; Bu, X.; Wang, B.; Feng, P. *Science* **2002**, *298*, 2366–2369.
- (7) (a) Zheng, N.; Bu, X.; Vu, H.; Feng, P. *Angew. Chem.* **2005**, *117*, 5433–5437; (b) *Angew. Chem., Int. Ed.* **2005**, *44*, 5299–5303.
- (8) (a) Wang, C.; Bu, X.; Zheng, N.; Feng, P. *Chem. Commun.* **2002**, 1344–1345. (b) Vaqueiro, P. *Inorg. Chem.* **2008**, *47*, 20–22.
- (9) (a) Wang, C.; Bu, X.; Zheng, N.; Feng, P. *Angew. Chem.* **2002**, *114*, 2039–2041; (b) *Angew. Chem., Int. Ed.* **2002**, *41*, 1959–1961.
- (10) Zhou, J.; Dai, J.; Bian, G.-Q.; Li, C.-Y. *Coord. Chem. Rev.* **2009**, *253*, 1221–1247.
- (11) (a) Li, J.; Chen, Z.; Emge, T. J.; Proserpio, D. M. *Inorg. Chem.* **1997**, *36*, 1437–1442. (b) Zhou, J.; Zhang, Y.; Bian, G.-Q.; Zhu, Q.-Y.; Li, C.-Y.; Dai, J. *J. Cryst. Growth Des.* **2007**, *7*, 1889–1892. (c) Chen, X.; Huang, X.; Li, J. *Inorg. Chem.* **2001**, *40*, 1341–1346.
- (12) (a) Wang, Y.-H.; Luo, W.; Jiang, J.-B.; Bian, G.-Q.; Zhu, Q.-Y.; Dai, J. *Inorg. Chem.* **2012**, *51*, 1219–1221. (b) Zhang, Q.; Chung, I.; Jang, J. I.; Ketterson, J. B.; Kanatzidis, M. G. *Chem. Mater.* **2009**, *21*, 12–14.
- (13) Franke, E. R.; Schäfer, H. *Z. Naturforsch., B* **1972**, *27*, 1308–1315.
- (14) Sheldrick, G. M. *Acta Crystallogr.* **2008**, *A64*, 112–122.
- (15) Spek, A. L. *Acta Crystallogr.* **2009**, *D65*, 148–155.
- (16) Campbell, J.; Dixon, D. A.; Mercier, H. P. A.; Schrobilgen, G. J. *Inorg. Chem.* **1995**, *34*, 5798–5809.
- (17) Zhou, J.; Zhang, Y.; Bian, G.-Q.; Zhu, Q.-Y.; Li, C.-Y.; Dai, J. *Cryst. Growth Des.* **2007**, *7*, 1889–1892.



- (18) (a) Li, J.; Chen, Z.; Emge, T. J.; Proserpio, D. M. *Inorg. Chem.* **1997**, *36*, 1437–1442. (b) Wang, C.; Haushalter, R. C. *Inorg. Chem.* **1997**, *36*, 3806–3807.
- (19) Srinivasan, B. R.; Naik, A. R.; Poisot, M.; Näther, C.; Bensch, W. *Polyhedron* **2009**, *28*, 1379–1385.
- (20) Blatov, V. A. *IUCr CompComm Newsletter* **2006**, 4–38.
- (21) Heller, G. *Top. Curr. Chem.* **1986**, *131*, 39–98.
- (22) Liebau, F. *Structural Chemistry of Silicates*; Springer: Berlin, Germany, 1985.
- (23) (a) Zeuner, M.; Pagano, S.; Schnick, W. *Angew. Chem.* **2011**, *123*, 7898–7920; (b) *Angew. Chem., Int. Ed.* **2011**, *50*, 7754–7775.
- (24) (a) Dehnen, S.; Brandmayer, M. K. *J. Am. Chem. Soc.* **2003**, *125*, 6618–6619. (b) Melullis, M.; Clérac, R.; Dehnen, S. *Chem. Commun.* **2005**, 6008–6010. (c) Ruzin, E.; Fuchs, A.; Dehnen, S. *Chem. Commun.* **2006**, 4796–4798. (d) Ruzin, E.; Dehnen, S. *Z. Anorg. Allg. Chem.* **2006**, *632*, 749–755. (e) Haddadpour, S.; Melullis, M.; Staesche, H.; Mariappan, C. R.; Roling, B.; Clérac, R.; Dehnen, S. *Inorg. Chem.* **2009**, *48*, 1689–1698. (f) Kaib, T.; Haddadpour, S.; Kapitein, M.; Bron, P.; Schröder, C.; Eckert, H.; Roling, B.; Dehnen, S. *Chem. Mater.* **2012**, *24*, 2211–2219.
- (25) Ewald, B.; Huang, Y.-X.; Kniep, R. *Z. Anorg. Allg. Chem.* **2007**, *633*, 1517–1540.
- (26) Neumair, S. C.; Vanicek, S.; Kaindl, R.; Többens, D. M.; Martineau, C.; Taulelle, F.; Senker, J.; Huppertz, H. *Eur. J. Inorg. Chem.* **2011**, 4147–4152.
- (27) (a) Smith, D. M.; Ibers, J. A. *Coord. Chem. Rev.* **2000**, *200–202*, 187–205. (b) Huffman, J. C.; Haushalter, R. C. *Z. Anorg. Allg. Chem.* **1984**, *518*, 203–209. (c) Devereux, L. A.; Schrobilgen, G. J.; Sawyer, J. F. *Acta Crystallogr.* **1985**, *C41*, 1730–1733.
- (28) (a) Heine, J.; Dehnen, S. *Z. Anorg. Allg. Chem.* **2008**, *634*, 2303–2308. (b) Heine, J.; Dehnen, S. *Inorg. Chem.* **2010**, *49*, 11216–11222. (c) Sportouch, S.; Belin, C.; Tillard-Charbonnel, M. *Acta Crystallogr.* **1994**, *C50*, 1861–1862.
- (29) Isaenko, L.; Vasilyeva, I.; Yelisseyev, A.; Lobanov, S.; Malakhov, V.; Dovlitova, L.; Zondy, J.-J.; Kavun, I. *J. Cryst. Growth* **2000**, *218*, 313–322.
- (30) Badikov, V. V.; Chizhikov, V. I.; Efimenko, V. V.; Efimenko, T. D.; Panyutin, V. L.; Shevyrdyaeva, G. S.; Scherbakov, S. I. *Opt. Mater.* **2003**, *23*, 575–581.
- (31) Isaenko, L.; Krinitsin, P.; Vedenyapin, V.; Yelisseyev, A.; Merkulov, A.; Zondy, J.-J.; Petrov, V. *Cryst. Growth Des.* **2005**, *5*, 1325–1329.